Fabrication and Characterization of Biodegradable Poly(propylene Carbonate)/Wood Flour Composites

X. C. Ge,[1] Q. Zhu,[1] Y. Z. Meng,[1,2]

[1]Guangzhou Institute of Chemistry, Chinese Academy of Sciences, P.O. Box 1122, Guangzhou 510650, People's Republic of China
[2]Institute of Energy & Environment Materials, School of Physics & Engineering, Sun Yat-Sen University, Guangzhou 510275, People's Republic of China

ABSTRACT: Wood flour reinforced poly(propylene carbonate) (PPC) composites were prepared by melt blending followed by compression molding. The effects of reinforcement on the morphology, static and dynamic mechanical properties, and thermal properties of PPC/wood flour composites were investigated. In terms of mechanical properties, wood flour had the significant effect of improving tensile strength and stiffness. Scanning electron microscopic examination revealed good dispersion of wood flour (especially at lower content) in the PPC matrix. Moreover, experimental results indicated that the wood flour addition led to an obvious improvement in the thermal stability of the composites. This paper demonstrates that the incorporation of low-cost and biodegradable wood flour into PPC provides a practical way to produce completely biodegradable and cost-competitive composites with good mechanical properties. © 2005 Wiley Periodicals, Inc. J Appl Polym Sci 99: 782–787, 2006
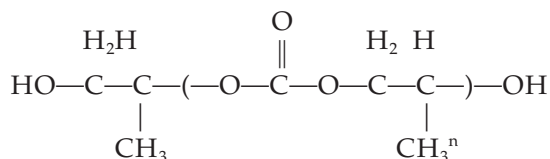
Key words: composites; polycarbonate; wood flour; biodegradable polymer; mechanical property

INTRODUCTION

Poly(propylene carbonate) (PPC), a new class of biodegradable polyesters synthesized from propylene oxide (PO) and carbon dioxide (CO_2), has been paid much attention due to several concerns for our environment and society.[1–4] CO_2 is massively released from modern large-scale industry and has a surplus increment of 10^9 tons per year in the earth. The increasing CO_2 results in serious effects on the environment, especially with respect to global warming.[5–7] On the other hand, such abundant CO_2, the amount of which is estimated to be more than the total amount of natural gas, petroleum, and coal stored in the earth, is an important substitute carbon resource and is in urgent need of being exploited. Most currently used polymeric materials, mainly alkane derived, show undegradability and may have a lifetime of over a hundred years when buried in typical solid waste sites. Growing environmental concerns have created an urgent need to develop new biodegradable materials that have comparable properties with today's polymeric materials at an equivalent cost.

More recently, PPC was synthesized by the reaction of CO_2 with PO using supported catalyst in very high yield (126 g polymer/g catalyst) in our laboratory. The catalyst was synthesized from zinc oxide and glutaric acid under magnetic stirring, followed by supporting on different materials.[8,9] Such PPC possesses an alternating molecular structure as shown below and exhibits superior mechanical strength, reasonable melt processability, high transparency, and good biodegradability in surroundings of both soil and buffer solution.[8–10]

$$\text{HO} - \overset{\displaystyle H_2}{\underset{\displaystyle CH_3}{C}} - \overset{\displaystyle H}{C} - (-O - \overset{O}{\overset{\|}{C}} - O - \overset{\displaystyle H_2}{C} - \overset{\displaystyle H}{\underset{\displaystyle CH_3}{C}} -)_n - \text{OH}$$

The use of cellulose-based fillers such as wood flour, wood fibers, and cellulose fibers in polymeric composites has grown extremely rapidly during the past years. This is because they are inexpensive, abundant, biodegradable, renewable, and environmen-

tally friendly.[11–13] Moreover, characterized by low density and hardness, together with high stiffness and strength, these fillers offer a number of advantages over the currently used inorganic reinforcements (e.g., glass fibers, calcium carbonate, mica), including flexibility during processing with no harm to the processing equipment.[14,15]

Wood is composed primarily of cellulose, a linear polymer of β-1,4-linked glucose units, and lignin, a three-dimensional amorphous natural polymer containing phenylpropane units tri- or tetra- substituted with hydroxyl and metoxyl groups, and hemicellulose.[16] Because of the structures aforesaid, wood flour or wood fiber exhibits a highly polar and hydrophilic nature. In previous work,[17] unmodified starch was simply melt blended with biodegradable PPC, and the results showed that the incorporation of a certain content of starch significantly improved the stiffness, tensile strength, and thermal stability of the composites. Wood fiber is similar to starch in several aspects, e.g., they all have large amount of glucose units. Thus, wood flour is expected to have a positive effect when blended with PPC. Moreover, since wood flour shows hydrophilic behavior, it is anticipated that its incorporation can greatly increase the water absorption of PPC, thereby enhancing the biodegradation properties. In these regards, the main aim of this work is to develop a kind of completely biodegradable and cost-competitive PPC/wood flour composite with applicable mechanical properties.

EXPERIMENTAL

Materials

The PPC used in this work was synthesized in our laboratory with a number-average molecular weight of 88,100 and polydispersity of 2.53. The wood flour (WF) used was typical bamboo flour (belongs to species of *Sinarundinaia nitida nakai*) obtained from a local supplier in the Guangdong Province of China. The particle size of WF was 120 mesh. PPC pellets and WF were vacuum dried at 75 °C for > 48 h prior to compounding.

Preparation of composites

Composites with PPC/WF weight ratios of 90/10, 80/20, 70/30, and 60/40 were prepared in a Brabender Plasticorder batch mixer at 150°C and a rotary speed of 60 rev min⁻¹ for 6 min. The chamber volume was 50 cm³. For each sample, 50 g of material was fed into the batch. Melt torque of the composites was recorded during the mixing period. For the purpose of comparison, pure PPC was also melt blended under similar processing conditions in the mixer. The composites subject to blending were stored in a tightly sealed vial

to prevent any moisture absorption. The mixtures were melt pressed into sheets 1 mm thick and then cut into standard dog-bone tensile bars (ASTM D638) with dimensions of $25 \times 4 \times 1$ mm³.

Mechanical properties

The static tensile properties were measured at 23°C and relative humidity of $50 \pm 5\%$ using an Instron Model 5566 tensile tester. The cross-head speed was set at 10 mm min⁻¹. Five specimens of each sample were tested, and the average results were reported. Prior to measurements, the samples were conditioned at 23 °C and $50 \pm 5\%$ humidity for 24 h by placing them in a closed chamber containing a saturated $C_a(NO_3) \cdot 4H_2O$ solution in distilled water (ASTM E-104). Dynamic mechanical analysis (DMA) was carried out with a Du Pont DMA (model 983) at a fixed frequency of 1 Hz and an oscillation amplitude of 0.2 mm. The dimension of the specimens used was $30 \times 10 \times 1$ mm³. The temperature of the specimens employed ranged from -50 to 100 °C at a heating rate of 2°C/min.

Fourier transform infrared spectroscopy measurements

Fourier transform infrared spectroscopy (FTIR) spectra were recorded in a Bruker Vector 22 FTIR spectrometer. The frequency range of FTIR was 4000–500 cm⁻¹ with resolution of 4.0 cm⁻¹ and scan rate of 8 scans/s. Samples were measured in the form of thin films ~60 μm thick, which were prepared by hot press molding.

Thermogravimetric analyses

Thermogravimetric analysis (TGA) measurements of the samples were performed in a Perkin-Elmer TGA-6 under a nitrogen protective atmosphere. The temperature used ranged from 50 to 500°C with a heating rate of 20 °C/min. Prior to the analysis, the samples were dried in a vacuum oven at 75 °C for 24 h.
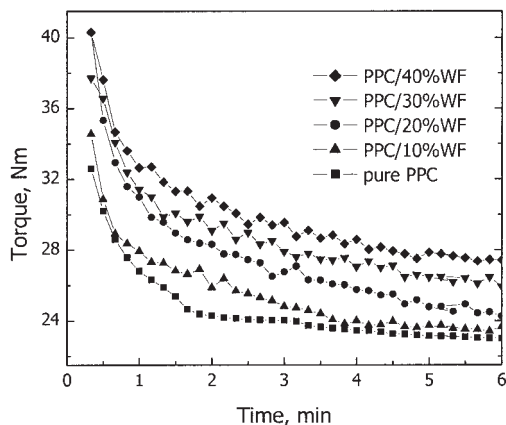
Morphology observation

The tensile bars were room-temperature fractured and used for morphology observation with a scanning electron microscope (Hitachi S-520) operated at 20 kV. Prior to the examination, the fractured surfaces were coated with a thin layer of gold.

RESULTS AND DISCUSSION

Torque behavior

Figure 1 shows the typical torque curves for the pure PPC and PPC/WF composites measured using the
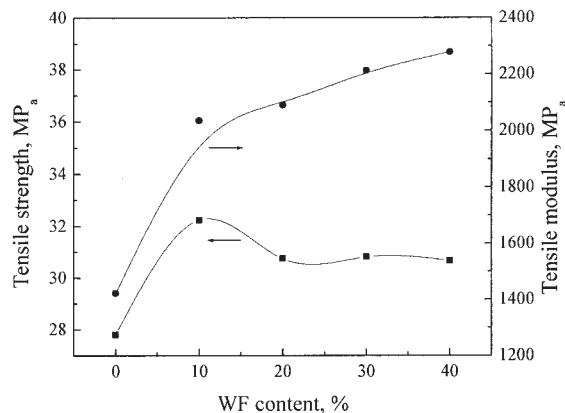
Figure 1 Torque value versus mixing time for pure PPC and PPC/WF composites.

Figure 2 Variations of tensile strength and modulus for PPC/WF composites with wood flour content.

Brabender Plasticorder with mixer attachment. The torque value of melt polymer is considered to be associated with the melt viscosity and consequently with the processability of the composite. All torque–time curves reached a high value of ~36 Nm within the first minute upon feeding materials into the mixer batch. This is due to the initial melting of the PPC matrix. Beyond this point, torque decreased gradually, caused by complete melt of PPC and frictional heating, until a relatively equilibrium torque value, which corresponds to an equilibrium viscosity. According to previous work,[18] high-molecular-weight PPC may suffer chain unzipping decomposition or chain scission decomposition at a certain temperature. Thus, the melt blending duration was controlled as short as possible, for instance, within 6 min in this work.

Regarding the steady-state torque values measured at a blending time of 6 min, it is apparent that the melt viscosities increased with increasing WF content. This is a common rule for fiber-filled composites. The short fibrous WF with irregular shape in the composites can perturb the normal flow of polymer melt and hinder the mobility of polymer chain segments in the flow. Furthermore, the fiber–fiber collisions also increase the melt viscosity with increasing fiber loading.[11]

Mechanical properties

The incorporation of wood fibers in thermoplastics generally, and in polyolefins in particular, leads to a lower tensile strength, which results from the poor interfacial bonding between the hydrophilic WF and the hydrophobic polymer matrix.[19,20] Chemical modifications of the surface of WF with various coupling agents and compatibilizers are usually adopted to afford satisfactory mechanical properties.[21–23] In the case of this study, unmodified WF was simply melt blended with biodegradable PPC. The variations of tensile strength, elongation at break, and tensile mod-

ulus of the PPC composites with WF content are presented in Figures 2 and 3, respectively. It can be seen from Figure 2 that the tensile strength increased initially when 10 wt % content of WF was added, with a significant increment of 16.0%. With increasing WF content from 10 to 20 wt %, the tensile strength decreased dramatically. The results mainly resulted from the decrease of the interfacial adhesion and homogeneity with increasing WF loading, because the filler particles tended to form agglomerates due to the presence of lignin and OH group in cellulose. These agglomerates then behave as bigger particles, reducing the effective adhesion surface.[24] The tensile strengths of the composites do not vary significantly with further increasing WF fraction up to 40 wt %, and their values were about 10.0% more than that of pure PPC. The results indicated that WF had a significant reinforcement effect on PPC/WF composites. The tensile modulus of PPC/10%WF composite dramatically increased compared with neat PPC. Upon further increasing the WF content from 10 to 40 wt %, the tensile
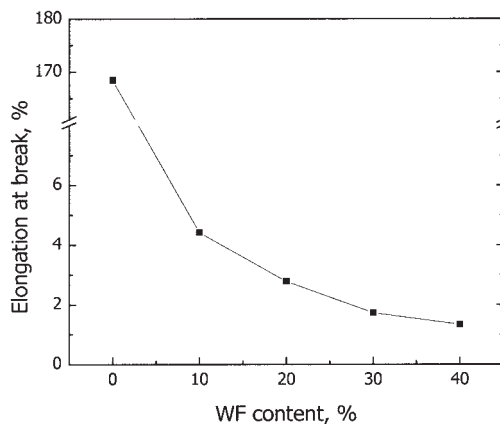
Figure 3 Elongation at break versus wood flour content for PPC/WF composites.
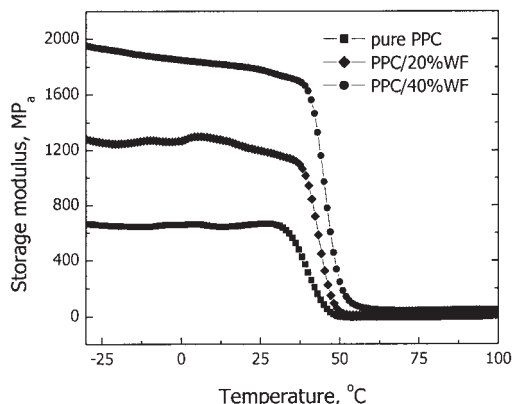
Figure 4 Storage modulus versus temperature for PPC and PPC/WF composites.

TABLE I
Thermal Properties of Pure PPC and PPC/WF Composites

Specimen	T_g (°C)	$T_{-5\%}$ (°C)	T^1_{max} (°C)	T^2_{max} (°C)
Pure PPC	43.8	248.1	265.9	—
PPC/10%WF	53.2	269.5	283.6	—
PPC/20%WF	52.7	270.8	282.1	—
PPC/30%WF	53.4	270.6	281.0	337.6
PPC/40%WF	53.7	271.3	282.1	339.4
Wood flour	—	262.2	—	347.1

modulus of the composites increased almost linearly. The fact resulted from the stiffening effect of WF within the PPC matrix because the modulus of WF is higher than that of PPC. Fillers with greater stiffness than the matrix can certainly increase the modulus of composites, but generally cause a dramatic decrease in the elongation at break.[19] As can be seen from Figure 3, the composites became brittle upon the addition of wood flour.

The storage modulus and tanδ versus temperature curves of the typical composites and pure PPC are depicted in Figures 4 and 5, respectively. As expected, storage modulus decreased with increasing temperature, with the most rapid reduction occurring at ~50 °C, corresponding to glass transition temperature (T_g) for PPC. Moreover, the storage modulus appeared to increase with increasing WF content over the whole measurement temperature, which is in accordance with the tensile modulus measurement. From Figure 5, it is obvious that T_g, as identified by the tan_δ peak, shifted to higher temperature in the composites. This
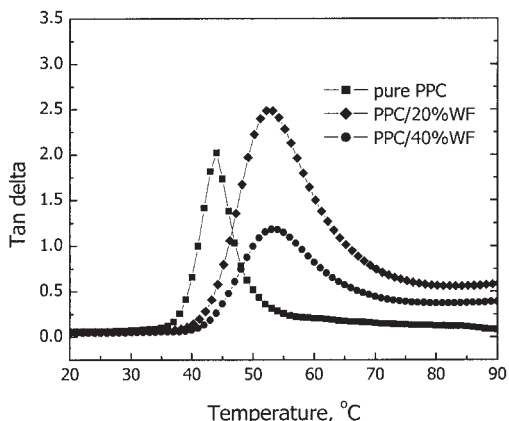
is because the mobility of PPC molecular chains was restricted by WF; it is also due to the presence of an interaction between PPC and WF. In addition, the T_g showed no significant changes for the composites with different content of WF, as can be seen clearly from Table I.

Morphology observation

Figure 6 shows the FTIR spectra of pure PPC, WF, and typical PPC/30% WF composite. In previous work,[17] unmodified starch was melt blended with PPC and the existence of hydrogen bondings between carbonyl groups of PPC and hydroxyl groups of starch was proved by FTIR spectra. For this case, the absorption peak at 1752 cm^{-1} for pure PPC, corresponding to C = O groups, became weaker and shifted obviously to a smaller wavenumber (1744 cm^{-1}) in the PPC/30% WF composite. Meanwhile, it is observable that the peak at 3414 cm^{-1} attributed to –OH groups for WF shifted to a smaller wavenumber compared with that for PPC/30% WF (3410 cm^{-1}). The results provided direct proof for the interaction between carbonyl

Figure 5 Tanδ versus temperature for PPC and PPC/WF composites.
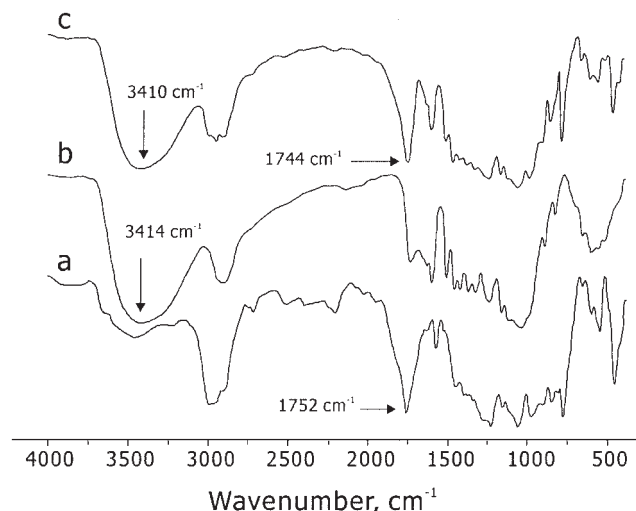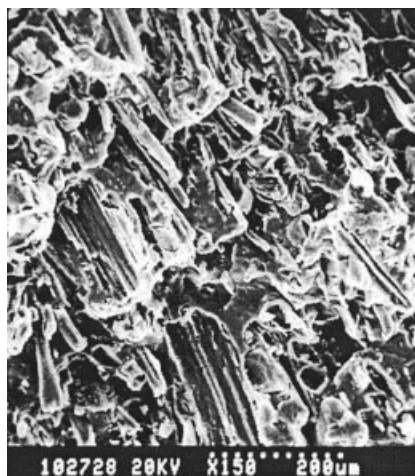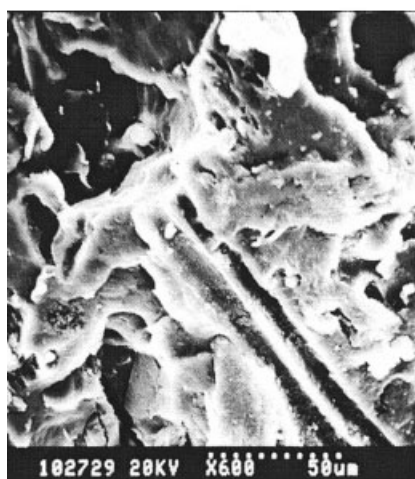

**Figure 6** FTIR spectra of (a) pure PPC, (b) wood flour, and (c) PPC/30%WF composite.

(a)

(b)

Figure 7 SEM micrographs for PPC/20% WF composite at magnifications of (a) 150× and (b) 600×.

groups of PPC and hydroxyl groups of WF via hydrogen bondings, which contributed to the reinforcement effect of WF on PPC/WF composites.

Examination of the fracture surfaces of the composites by scanning electron microscope (SEM) gave further information about the morphology of PPC/WF composites. The SEM micrographs of PPC/20% WF and PPC/40% WF composites are shown in Figures 7(a,b) and 8, respectively. Figure 7(a) shows good dispersion of WF particles within the PPC matrix. From Figure 7(a,b), one can see that the WF had the shape of irregular short fibers with coarse surface in the composite, which can provide better adhesion between the fillers and polymer matrix. In addition, the longer wood fibers tend to align along the melt flow direction as shown in Figure 7(a). The phenomena aforementioned were expected to have positive effects on the mechanical properties of the composites. However, there
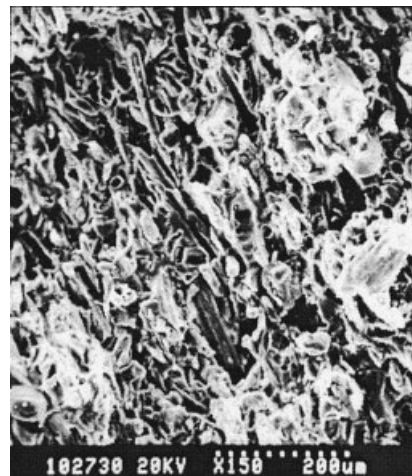

**Figure 8** SEM micrographs for PPC/40% WF composite.

existed gaps around the WF particles and voids where WF particles were pulled out, indicating the immiscibility between the polymer and WF fillers. For PPC/40% WF composite, more and larger agglomerates than in PPC/20% WF can be observed (Fig. 8). This explained why PPC/40% WF had a lower tensile strength than PPC/20% WF. Moreover, it is difficult to find the alignment of the wood fibers within the PPC matrix from Figure 8. This resulted from the fiber–fiber collision with increasing fiber loading. In addition, micrographs in Figure 7(a,b) and 8 show that the fracture of filler-reinforced composites occurred in two ways: fiber/matrix debonding and fiber pull-out.

Thermal behavior

TGA was employed to study the thermal decomposition characteristics of the composites. The 5% weight loss temperatures ($T_{-5\%}$) and the maximum weight loss temperatures (T_{max}) determined by DTG are
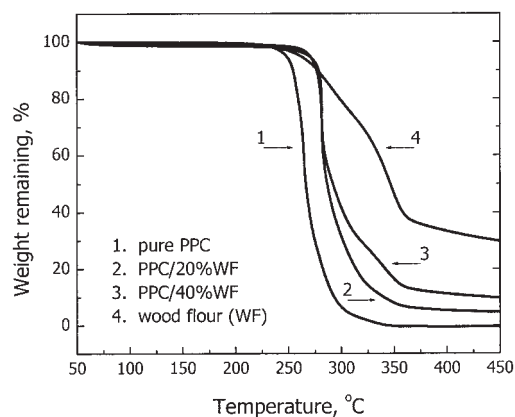
Figure 9 Thermogravimetric curves for PPC, wood flour, and PPC/WF composites.
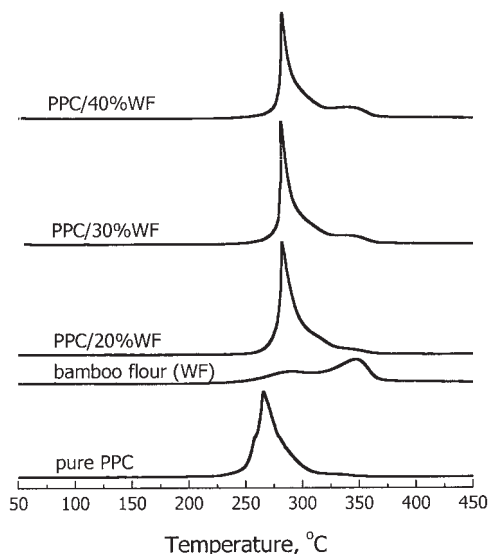
Figure 10 DTG curves for PPC, wood flour, and PPC/WF composites.

listed in Table I. The addition of WF led to a considerable increase in $T_{-5\%}$ for the composites by >20°C compared with that of pure PPC and ~10°C compared with that of wood flour. The results can be clearly observed in Figure 9. This demonstrated that the WF incorporation improved the thermal stability of PPC significantly. The thermal degradation process for the components and composites can be well illustrated by DTG curves, as shown in Figure 10. For pure PPC, only one intense decomposition stage, with a peak temperature at 265.9°C, can be observed. For wood flour, there existed two decomposition peaks: the relatively small peak (designed T^2_{max} in Table 1) at 347.1°C was attributed to cellulose decomposition, and the hardly detectable one at 292.6°C was thermal depolymerization of hemicellulose and the glycosidic linkages of cellulose.[25,26] By comparing DTG curves of the composites with those of pure PPC and WF, one can see that the profile of DTG curves for PPC/WF composites was not a simple merge of the DTG curves of PPC and WF. The decomposition peak of PPC/WF composites at 265.9°C for PPC phase shifted obviously to higher temperature, indicating that the addition of WF can increase the thermal stability of the PPC composites.

CONCLUSIONS

A series of WF reinforced PPC composites was prepared by melt blending. The morphology, static and dynamic mechanical behavior, and thermal properties were investigated. The tensile strengths of the com-

posites increased significantly with a maximum increment of 16.0% at 10 wt % wood flour addition. The stiffness of the composites was greatly enhanced with the introduction of WF. Thermal analysis indicated that the wood flour addition led to a significant improvement in thermal stability of the composites. The reinforcement in mechanical properties and the improvement in thermal properties resulted from the interaction between the carbonyl groups of PPC and the hydroxyl groups of wood flour via hydrogen bondings, as evidenced by FTIR investigation. Scanning electron microscopic examination revealed that WF particles were well dispersed within the PPC matrix at lower filler loading, and meanwhile, longer wood flour tended to align along the melt flow direction.

References

1. Gorecki, P.; Kuran, W. J Polym Sci Polym Lett Ed 1985, 23, 299.
2. Nishimura, M.; Kasai, M.; Tsuchida, E. Makromol Chem 1978, 179, 1913.
3. Tsuchida, E.; Kasai, M. Makromol Chem 1980, 181, 1612.
4. Chen, X.; Shen, Z.; Zhang, Y. Macromolecules 1991, 24, 5305.
5. Kacholia, K.; Reck, R. A. Clim Chan 1997, 35, 53.
6. Broecker, W. S. Science 1997, 278, 1582.
7. Meehl, G. A.; Washington, W. M. Nature 1996, 382, 56.
8. Wang, S. J.; Tjong, S C.; Du, L. C.; Zhao, X. S.; Meng, Y. Z. J Appl Polym Sci 2002, 85, 2327.
9. Zhu, Q.; Meng, Y. Z.; Tjong, S. C.; Zhao, X. S.; Chen, Y. L. Polym Int 2002, 51, 1079.
10. Meng, Y. Z.; Du, L. C.; Tjong, S. C.; Zhu, Q.; Hay, A. S. J Polym Sci, A Polym Chem 2002, 40, 3579.
11. George, J.; Janardhan, R. J.; Anand, J. S.; Bhagawan, S. S.; Thomas, S. Polymer 1996, 37, 5421.
12. Karmaker, A. C.; Youngquist, J. A. J Appl Polym Sci 1996, 62, 1147.
13. Coutinho, F. M. B.; Costa, T. H. S.; Carvalho, D. L. J Appl Polym Sci 1997, 65, 1227.
14. Park, B. D.; Balatinecz, J. J Polym Compos 1997, 18, 79.
15. Kim, T. J.; Lee, Y. M.; Im, S. S. Polym Compos 1997, 18, 273.
16. Feldman, D.; Banu, D. J Appl Polym Sci 1997, 66, 1731.
17. Ge, X. C.; Li, X. H.; Zhu, Q.; Li, L.; Meng, Y. Z. Polym Eng Sci, 2004, 44, 2134.
18. Li, X. H.; Meng, Y. Z.; Zhu, Q.; Tjong, S. C. Polym Degrad Stabil 2003, 81, 157.
19. Oksman, K.; Clemons, C. J Appl Polym Sci 1998, 67, 1503.
20. Dalväg, H.; Klason, C.; Strömvall, H. E. Intern J Polym Mater 1985, 11, 9.
21. Raj, R. G.; Kokta, B. V.; Maldas, D.; Daneault, C. J Appl Polym Sci 1989, 37, 1089.
22. Dong, S.; Sapieha, S.; Schreiber, H. P. Polym Eng Sci 1993, 33, 342.
23. Joseph, K.; Thomas, S.; Pavithran, C. Polymer 1996, 37, 5139.
24. Albano, C.; Ichazo, M.; González, J.; Delgado, M.; Poleo, R. Mater Res Innovat 2001, 4, 284.
25. Fung; K. L.; Li, R. K. Y.; Tjong, S. C. J Appl Polym Sci, 2002, 85, 169.
26. Albano, C.; González, J.; Ichazo, M.; Kaiser, D. Polym Degrad Stabil 1999, 66, 179.